

Research of the Possibility to Obtain Structures with Nanometer Layer Thicknesses and Sharp-Cut Interfaces between Them Using Ion-Beam and Reactive Ion-Beam Deposition Processes

A. A. Dedkova^{a,*}, V. Yu. Kireev^a, A. S. Myslivets^b, P. A. Rozel^b, and A. Yu. Trifonov^{a, c}

^a National Research University of Electronic Technology, Moscow, 124498 Russia

^b Izovac Ltd., Minsk, 220075 Belarus

^c Lukin Scientific Research Institute of Physical Problems, Moscow, 124460 Russia

*e-mail: dedkova@ckp-miet.ru

Received March 6, 2019; revised July 21, 2019; accepted September 20, 2019

Abstract—At present, atomic layer deposition and magnetron sputtering processes are used in the production of integrated circuits (IC) to obtain structures with nanometer layer thicknesses and sharp interfaces between them. However, there are also ion-beam and reactive ion-beam deposition processes, which are mainly used to produce multilayer optical coatings. The aim of this work is to study the possibility of obtaining structures with nanometer layer thicknesses and sharp interfaces between them in the processes of ion-beam and reactive ion-beam deposition. The studies were carried out by time-of-flight secondary ion mass spectrometry (SIMS) and spectral ellipsometry methods. Study of the structure Ta (3 nm)/Nb (3 nm)/Ta (3 nm) reveals that ion-beam deposition can form structures with nanometer layer thicknesses and sharp boundaries between them. On the other hand, in reactive ion-beam deposition of the structure Nb (3 nm)/Ta₂O₅ (3 nm)/Nb (3 nm), oxidation occurs on the entire thickness of the metal layer following the metal oxide layer due to ions, atoms, and molecules of oxygen contained in the ion beam.

DOI: 10.1134/S1995078019030042

INTRODUCTION

In 2018, global microelectronics saw the beginning of the mass production of advanced products: integrated circuits (ICs), which include microprocessors and memory devices with a minimum size of 11/10 nm [1, 2]. Pilot lines of leading microelectronic companies, such as Intel, Samsung, TSMC and AMD, have demonstrated the possibility of manufacturing advanced products with a minimum size of 7 nm [3, 4].

Simultaneously with the decrease in the minimum horizontal-plane dimensions, the thickness of the functional layers of microelectronic products has also decreased to the nanometer level, in particular:

- gate dielectrics of CMOS transistors [5];
- barrier and adhesive copper-metallization layers [6];
- semiconductor layers of epitaxial heterostructure lasers [7];
- magnetic, metal, and dielectric layers of IC non-volatile magnetic random access memory (magnetic RAM) on spin transfer torque STT-MRAM) [8].

In microelectronics production, atomic-layer deposition (ALD) processes are used to obtain structures with nanometer layer thicknesses and sharp interfaces between them [9], varieties of which are

atomic layer epitaxy (ALE) [10] and magnetron sputtering processes [11], which includes reactive magnetron sputtering [12].

In [5], SiO₂ and HfO₂ layers with nanometer thickness were deposited in the formation of MOS transistor gate assemblies, the first on a silicon substrate, and the second on silicon oxide by ALD; a set of sequentially deposited MgO, CoFeB, and Ta nanometer films for the manufacture of STT-MRAM memory devices was created in [13] using magnetron sputtering.

ALD processes are the most preferred and controllable for attaining layers of nanometer thickness with a sharp boundary between. In ALD processes, cyclic discrete chemical reactions result in layerwise (one atomic layer of material per cycle) deposition of a film made from two precursors (reagents) fed to the reactor sequentially after its pumping (purging) stages. Therefore, to obtain a film with the required thickness, it is sufficient to set the desired number of deposition cycles.

Unfortunately, at present, the necessary precursors (reagents) do not exist for all materials used in microelectronics production, in particular, those consisting of two or more compounds [9].

Film deposition by magnetron sputtering employs the universal process of physical sputtering of atoms or molecules of materials of targets in reduced-pressure gas discharge plasma with using accelerated ions of an inert gas, usually argon. If targets of the required materials are available, films with these materials can be obtained.

For targets from dielectric materials, radio or high-frequency (RF) generators are used and magnetron sputtering in this case is called RF magnetron sputtering. If there are no RF generators in the magnetron system, films of dielectric materials, usually metal oxides, can be obtained by sputtering metal targets in argon and oxygen plasma. In this case, oxygen atoms and ions will oxidize metal atoms on the target, in the discharge plasma, and on the surface of the substrate during film formation. Such a process is called reactive magnetron sputtering [12].

Although the magnetron and reactive magnetron sputtering processes are quite simply realized using magnetron sputtering systems, the operating parameters for producing nanometer films with sharp interfaces between them lie within very narrow technological ranges. This is due to the characteristics of magnetron sputtering systems.

In magnetron discharges, it is impossible to independent monitoring the density of the ion current to the target and the energy of the ions bombarding the target. Therefore, the rate of sputtering of the target and, accordingly, the rate of deposition of the film on the substrate is determined by the power of the magnetron discharge. The magnetron discharge exists in a rather narrow range of working pressures of the gas. It lights up at a sufficiently high minimum power, at which the target sputtering rates and deposition rates of films on the substrate are sufficiently high, which makes it difficult to control the thickness of films, especially in the nanometer range [11, 12].

The energy of the sputtered particles of the target material, even at minimal magnetron discharge powers, is several electron-volts [11], which leads to mixing of the atoms of the substrate surface and makes it difficult to obtain films with sharp interface boundaries. To reduce the energy of the sputtered particles in magnetron systems, the substrate holder is placed as far as possible from the sputtering targets. However, due to collisions of sputtered particles with molecules of residual gases (nitrogen, oxygen and water vapor) and due to the longer exposure of the latter to the substrate surface, contamination may occur, and the structure and composition of the deposited films may change.

Thus, deposition of films with nanometer thickness and sharp interfaces using magnetron sputtering is a complex technological problem; it is even more difficult for reactive magnetron sputtering processes.

Ion-beam deposition systems have wider technological capabilities and operate in a wider pressure

range than magnetron systems, since ion beams are generated in chambers of autonomous ion sources that can independently regulate the density and energy of the ion current [11]. Ion beams are directed to a vacuum chamber in which the targets and substrate holders with plates are placed; the beams sputter the target materials. Sputtered particles (atoms or molecules) of the targets in the vacuum chamber are deposited on the surface of the substrates and form the desired film.

Neutralized or electrically compensated ion beams are used to sputter dielectric targets in ion-beam deposition processes [1]. If ion-beam deposition systems do not have devices to neutralize or compensate for the electric charge of ion beams, or the levels of neutralization and compensation are insufficient to sputter dielectric targets, metal targets and beams of argon and oxygen ions are used for deposition dielectric films, such as metal oxides. Oxygen ions allow the metal material of target to be oxidized as well as sputtered with argon ions; therefore, a metal oxide film is deposited to the substrate surface. This process is called reactive ion-beam deposition [12, 14].

Since ion-beam deposition systems are hardly used in microelectronics production, the aim of this work is to study the possibility of obtaining structures with nanometer layer thicknesses and sharp interfaces between them using ion-beam and reactive ion-beam deposition processes.

EXPERIMENTAL

The experiments were performed on an Aspira 150 ion-beam deposition tool manufactured by Izovak LLC (Belarus), designed for deposition stable precision optical coatings [15]. Figure 1 shows a diagram inside the chamber apparatus of the Aspira 150 tool.

Before deposition processes, the working chamber was pumped out by oil-free fore vacuum and turbomolecular pumps to a residual pressure of 1×10^{-3} Pa. The tool is equipped with two ion-beam sources with compensators for the electric space charge of the ion beam: one ion source for cleaning the substrate surface and the other for sputtering the target.

The target assembly is equipped with a magazine for six interchangeable targets of various materials. The distance between targets and substrates during the ion-beam and reactive ion-beam deposition was 150 mm.

The substrate was pressed against the water-cooled substrate holder with a clamping ring, and helium was supplied to the space between the substrate and substrate holder to ensure good heat removal. The temperature of the substrate during ion cleaning and ion-beam deposition was 60°C.

Boron doped silicon wafers with resistivity of $12 \Omega \text{ cm}$, orientation (100), diameter of 150 mm and a 0.6- μm -thick thermal oxide layer on their surfaces were used as substrates. Before deposition, the sur-

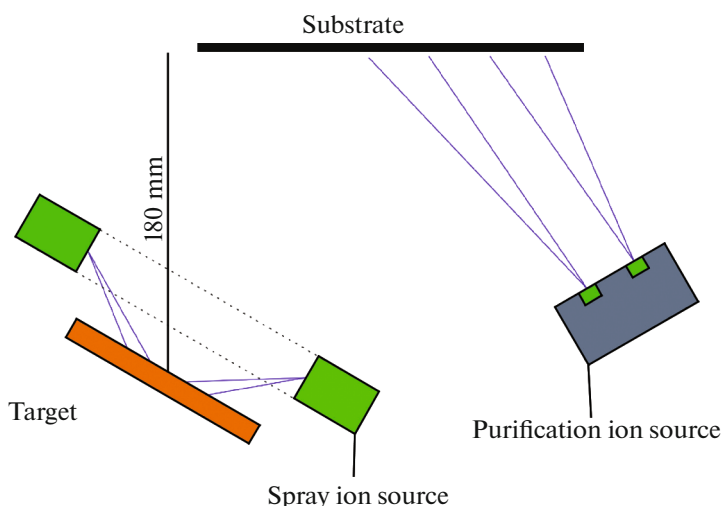


Fig. 1. (Color online) Diagram of inside of Aspira 150 working chamber.

faces of substrates were cleaned by ion beam. The deposition time of the layer was determined by measuring the deposition rate by changing the resonant frequency of the quartz sensor installed in the vacuum chamber.

During ion-beam deposition, the structure Ta (3 nm)/Nb (3 nm)/Ta (3 nm) was deposited to the substrate. Table 1 shows the modes of ion cleaning of the substrate and ion-beam deposition for this structure.

During reactive ion-beam deposition, Nb (3 nm)/Ta₂O₅ (3 nm)/Nb (3 nm) structure was deposited on the substrate. Table 2 shows the modes of ion cleaning of the substrate and ion-beam deposition for this structure.

Each of the two studied multilayer structures Ta (3 nm)/Nb (3 nm)/Ta (3 nm) and Nb (3 nm)/Ta₂O₅ (3 nm)/Nb (3 nm) was formed on five substrates.

To study the depth distribution profiles of elements in the obtained multilayer structures, time-of-flight secondary-ion mass spectrometry (SIMS) method was used. Despite the high energy of the analytical beam, due to the using pulsed mode the current of the analytical beam and the dose introduced during analysis are negligible. As a result, the depth resolution is

determined by the sputtering beam energy, which can be as low as several hundred electron-volts.

Modern time-of-flight spectrometers have a depth resolution of about 1 nm [16]; therefore, the target value of the layer thicknesses in the resulting multilayer structures was sensor-set to a thickness of 3 nm. The specific choice of three-layer structures of these materials was determined by the authors' projects on manufacturing supercapacitors and barrier layers for copper metallization [14].

In this study was used time-of-flight mass spectrometer SIMS 5-100 manufactured by ION TOF (Germany) with optimal depth resolution <1 nm [17].

The samples of the obtained Ta (3 nm)/Nb (3 nm)/Ta (3 nm) and Nb (3 nm)/Ta₂O₅ (3 nm)/Nb (3 nm) multilayer structures were analyzed in the TOF.SIMS 5-100 system under the following conditions:

—Bi⁺ analyzing beam with a current of 1.5 pA, an energy of 30 keV, and raster size of 100 × 100 μm;

—samples of multilayer structures were sputtered with O₂⁺ beam at an energy of 500 eV when analyzing positive secondary ions and with Cs⁺ beam at an energy of 500 eV when analyzing negative secondary ions; the raster dimensions were 300 × 300 μm;

Table 1. Modes of ionic substrate cleaning and ion-beam deposition of Ta (3 nm)/Nb (3 nm)/Ta (3 nm) structure on Aspira 150 device

Process	Working gas flow rate, cm ³ /min	Working pressure, Pa	Voltage of ion source, kV	Ion source current, mA	Processing time, s
	Ar				
Cleaning of substrate	10	0.06	1.0	40	120
Deposition of Ta	20	0.08	1.5	90	35
Deposition of Nb	20	0.08	1.5	90	35

Table 2. Modes of processes for ionic substrate cleaning and reactive ion-beam deposition of Nb (3 nm)/Ta₂O₅ (3 nm)/Nb (3 nm) structure on Aspira 150 device

Process	Working gas flow rate, cm ³ /min		Working pressure, Pa	Voltage of ion source, kV	Ion source current, mA	Processing time, s
	Ar	O ₂				
Cleaning of substrate	5.0	15	0.06	2.0	50	120
Deposition of Ta	21	0	0.11	3.0	70	50
Deposition of Nb	21	0	0.11	3.0	70	17
Deposition of Ta ₂ O ₅	11	60	0.17	3.8	90	25

—to calibrate the SIMS analysis signals of structural samples for the depth of the ion-sputtering crater, was used a Veeco Wyko NT9300 optical profiler in the phase-shifting interferometry mode, which made it possible to measure structures with small height differences [18].

For such measurements, the initial samples with ion-sputtering craters obtained during SIMS analysis were coated with a ~50-nm-thick Al layer using a sputtering tool TM-Magna 150 manufactured by public corporation NIITM (Russia) [19].

To compare the results of the thickness and layers characteristics analysis, the samples of multilayer Ta (3 nm)/Nb (3 nm)/Ta (3 nm) and Nb (3 nm)/Ta₂O₅ (3 nm)/Nb (3 nm) structures were also investigated with Horiba Auto SE and Horiba Uvisel 2 spectral ellipsometers. The spectral ellipsometry method was used to estimate the thickness and number of layers. For this purpose, optimization method was used [18] to process the obtained experimental ellipsometric

characteristics I_s and I_c related to ellipsometric parameters Ψ and Δ .

In particular, various model representations of the studied structures were used, which describe the presence or absence of each specific layer, its thickness, and optical characteristics [20]. Such a comprehensive analysis of the spectral ellipsometry results allowed conclusions to be drawn on the composition and thickness of the studied structures (see below).

RESULTS AND DISCUSSION

Figures 2 and 3 show the results of SIMS analysis of samples of two types of structures—Ta (3 nm)/Nb (3 nm)/Ta (3 nm) and Nb (3 nm)/Ta₂O₅ (3 nm)/Nb (3 nm)—in the form of the dependences of the ion current on the sputtering depth of the samples.

The dependencies in Figure 2 clearly show successive layers of Ta, Nb, and Ta with a thickness of 3 nm each. In SIMS, depth resolution is most often defined as the depth at which the signal from abruptly appear-

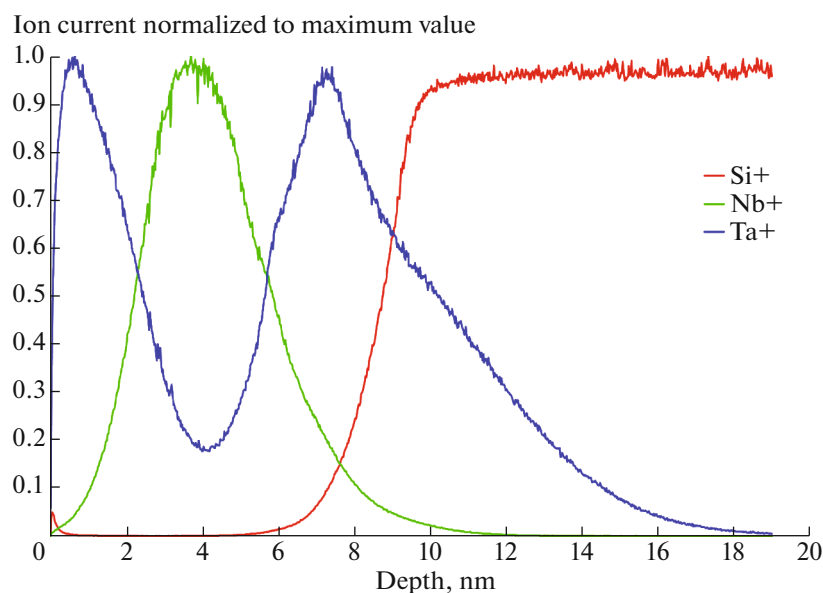


Fig. 2. (Color online) Dependences of ion current of main positive ions normalized to maximum value on sputtering depth of Ta (3 nm)/Nb (3 nm)/Ta (3 nm) structure with O₂⁺ ions at energy of 500 eV.

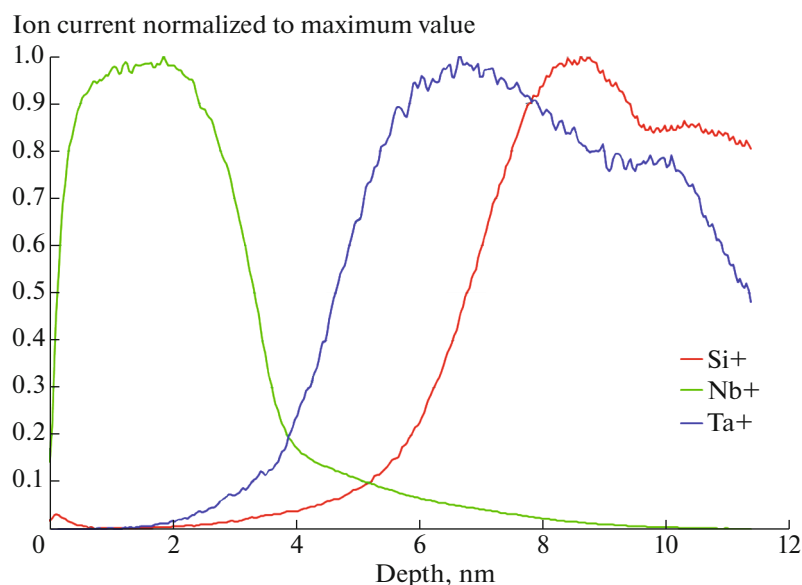


Fig. 3. (Color online) Dependences of ion current of main positive ions normalized to maximum value on sputtering depth of Nb (3 nm)/Ta₂O₅ (3 nm)/Nb (3 nm) structure with O₂⁺ ions at energy of 500 eV. The fixed oxygen level on this structure exceeds the dynamic range of the mass spectrometer, which proves the high degree of oxidation.

ing layer sharply increases from 16 to 84% of its maximum intensity. Using this criterion, the niobium profile indicates that the interface (or depth resolution) in this case is not more than 1.5 nm.

Ellipsometric studies of the Ta/Nb/Ta structure confirm that the two upper layers have a total thickness of about 6 nm. The boundary of the third layer (buried layer Ta) is not fixed against the background of an intense signal from 0.6 microns of silicon oxide substrate.

SIMS analysis of the sample with the Nb (3 nm)/Ta₂O₅ (3 nm)/Nb (3 nm) structure (Fig. 3) leads to the following conclusions:

- an extremely high oxygen signal is observed in the structure, which indicates a high degree of oxidation of the films contained in the structure;

- the structure contains an upper layer of niobium (Nb) with the specified thickness of 3 nm, but the interface between the upper Nb layer and Ta₂O₅ layer is almost completely blurred;

- in the structure there is a layer of tantalum oxide with a thickness of about 6 nm at a given thickness of 3 nm, and there is no buried layer of Nb with a given thickness of 3 nm.

There is no buried niobium layer because upon ion-beam deposition of the Ta₂O₅ layer, a partially ionized Ar/O₂ gas mixture with a percentage ratio of about 1 to 6 acts on the buried Nb layer (Table 2, last row). In such a mixture, the buried Nb layer is entirely oxidized by oxygen atoms and ions, and a layer of niobium oxide (Nb₂O₅) forms, which is observed during SIMS analysis.

The results of ellipsometric studies of the structure of Nb/Ta₂O₅/Nb show that:

- the thickness of the SiO₂ layer in the substrate areas under the Nb/Ta₂O₅/Nb structure is less than in the areas shielded by the pressure ring of the substrate holder without these coatings, which is due to the pre-ionic cleaning of the substrates with a gas mixture Ar/O₂ = 1/3 (Table 2, first row);

- there is a high degree of oxidation of niobium metal films contained in the structure;

- there is no well-defined buried Nb layer in the structure.

Thus, ellipsometric studies of the Nb/Ta₂O₅/Nb structure quite well support the results and conclusions of SIMS analysis.

The results of studying samples of multilayer structures from each plate were identical within the experimental error, which demonstrates the stability of the technological processing modes.

CONCLUSIONS

Based on experimental studies using time-of-flight secondary ion mass spectrometry and spectral ellipsometry, the following was shown for the first time:

- the ion beam deposition process in the mode shown in Table 1 makes it possible to obtain structures with layers with nanometer thickness and sharp boundaries between them;

- the reactive ion-beam deposition process in the mode shown in Table 2 does not yield structures with

layers with nanometer thickness and sharp boundaries between them due to oxidation of the entire thickness of the metal layers following the metal oxide layers, due to ions, atoms, and oxygen molecules contained in the ion beams.

FUNDING

The study was carried out with equipment of the Shared Research Center “Microsystem Technology and Electronic Component Base” of MIET with the support of the Russian Ministry of Science and Higher Education as part of contract no. 14.578.21.0250 (UN RFMEFI57817X0250).

CONFLICT OF INTEREST

The authors declare that they have no conflict of interest.

REFERENCES

1. V. Yu. Kireev, *Nanotechnology in Microelectronics. Nanolithography - Processes and Equipment* (Intellect, Dolgoprudnyi, 2016) [in Russian].
2. *International Roadmap for Device and Systems (IRDS), 2017 Ed., Executive Summary* (Inst. Electric. Electron. Eng. (IEEE), 2017).
3. AMD Navi GPU is Based on 7 nm Process. <https://fudzilla.com/news/graphics/43677-amd-navi-gpu-is-based-on-7nm-process>.
4. Design Norms in Microelectronics. www.nanonewsnet.ru/articles/2018/proektnye-normy-v-mikroelektronike-gde-na-samom-dele-7-nanometrov-v-tekhnologii-7nm. Accessed Sept. 24, 2018.
5. J. Robertson, “High dielectric constant gate oxides for metal gate Si transistors,” *Rep. Prog. Phys.* **69**, 327 (2006). <https://doi.org/10.1088/0034-4885/69/2/R02>
6. D. G. Gromov, A. I. Mochalov, A. D. Sulimin, and V. I. Shevyakov, *Ultra-Large Integrated Circuit Metallization* (BINOM, Moscow, 2012) [in Russian].
7. R. J. Martín-Palma, F. Agullo-Rueda, and J. Martínez-Duart, *Nanotechnology for Microelectronics and Optoelectronics* (Elsevier, Amsterdam, 2006; Tekhnosfera, Moscow, 2009).
8. UMC and Avalanche Technology Partner for MRAM Development and 28nm Production. <https://electroi.com/2018/08/umc-and-avalanche-technology-partner-for-mram-development-and-28nm-production>.
9. *Atomic Layer Deposition for Semiconductors*, Ed. by Ch. S. Hwang and Ch. Y. Yoo (Springer Science, New York, 2014).
10. A. L. Aseev, “Nanomaterials and nanotechnologies for modern semiconductor electronics,” *Russ. Nanotekhnol.* **1** (1–2), 97 (2006).
11. B. S. Danilin, *Application of Low-Temperature Plasma for Supplying Thin Films* (Energoatomizdat, Moscow, 1989) [in Russian].
12. E. V. Berlin and L. A. Seidman, *Production of Thin Films by Reactive Magnetron Sputtering* (Tekhnosfera, Moscow, 2014) [in Russian].
13. H. Sato, M. Yamanouchi, S. Ikeda, et al., “MgO/CoFeB/Ta/CoFeB/MgO recording structure in magnetic tunnel junctions with perpendicular easy axis,” *IEEE Trans. Magn.* **49**, 4437 (2013). <https://doi.org/10.1109/tmag.2013.2251326>
14. *Handbook of Semiconductor Interconnection Technology*, Ed. by G. C. Schwartz and K. V. Srikrishnan, 2nd ed. (CRC, Taylor Francis Group, New York, 2006).
15. Aspira 150. www.izovac.com.
16. P. van der Heide, *Secondary Ion Mass Spectrometry: An Introduction to Principles and Practices* (Wiley, New Jersey, 2014).
17. TOF.SIMS 5 - 100 brochure. www.iontof.com.
18. V. A. Shvets, E. V. Spesivtsev, S. V. Rykhliitskii, and N. N. Mikhailov, “Ellipsometry as a high-precision technique for subnanometer-resolved monitoring of thin-film structures,” *Nanotechnol. Russ.* **4**, 201 (2009).
19. MVU TM-Magna 150. www.niitm.ru.
20. A. A. Dedkova, V. Yu. Kireev, and N. S. Mazurkin, “Analysis of the parameters of the ferromagnetic films by means of the system for research of the magneto-optical effect of Kerr and a spectral ellipsometer,” *Nano-Mikrosist. Tekh.* **20**, 521 (2018). <https://doi.org/10.17587/nmst.20.521-527>